



Zain, A.R. M., and De La Rue, R.M. (2015) Control of coupling in 1D photonic crystal coupled-cavity nano-wire structures via hole diameter and position variation. *Journal of Optics*, 17(12), 125007. (doi:10.1088/2040-8978/17/12/125007)

This is the author's final accepted version.

There may be differences between this version and the published version. You are advised to consult the publisher's version if you wish to cite from it.

<http://eprints.gla.ac.uk/114795/>

Deposited on: 29 February 2016

# Control of coupling in one-dimensional (1D) photonic crystal coupled-cavity nano-wire structures via hole diameter and position variation

A R Md Zain<sup>1</sup> and R M.De La Rue<sup>2</sup>

<sup>1</sup>Institute of Microengineering and Nanoelectronics (IMEN), Universiti Kebangsaan Malaysia (UKM), 43600 UKM Bangi, Selangor, Malaysia.

<sup>2</sup>Optoelectronics Research Group, School of Engineering, University of Glasgow, Rankine Building, Oakfield Avenue, Glasgow G12 8QQ, Scotland, UK

[E-mail : rifqi@ukm.edu.my](mailto:rifqi@ukm.edu.my)

**Abstract:** We have successfully demonstrated close experimental control of the resonance splitting/free spectral range (FSR) of a coupled micro-cavity one-dimensional (1D) photonic crystal (PhC)/photonic wire (PhW) device structure based on silicon-on-insulator (SOI). Clear splitting of the resonances, with FSR values ranging from 8 nm to 48 nm, was obtained through the use of different hole arrangements within the middle section of the device structures, between the coupled cavities. The results show good agreement with calculations obtained using a finite-difference time-domain (FDTD) simulation approach.

## 1. Introduction

There has been a significant interest in realizing photonic integrated circuits (PIC) and sensors [1-3] by manipulating photonic crystal (PhC) cavity structures. The periodic structure of photonic crystals (PhCs) controls the optical propagation through a dielectric medium [4,5] - and provides a potential platform for realization of compact photonic biosensors and photonic integrated circuits (PICs) [6,7] with the aim of achieving monolithic integration on a single chip. Silicon-on-insulator (SOI) is one of the typical material systems used, due to its high refractive index contrast. This high contrast also makes it possible to achieve a large resonance quality factor (Q-factor) in a suitably designed structure - providing a promising candidate for sensing applications. Photonic crystal cavity structures can be optimized and designed in such a way that they demonstrate an extremely narrow resonance - where the resonance wavelength is particularly sensitive to changes induced by the deposition of biochemical material on the surface of the cavity. For example, in label-free detection, the cavity sensor operates by measuring changes in the wavelength of resonantly transmitted light as biochemical binding events take place on the surface. For bio-sensing applications, a cavity resonance Q-factor of approximately 5000 is sufficient since the propagation losses are mostly dominated by absorption in the water surrounding the waveguide - at operating wavelengths around 1.5  $\mu\text{m}$ , since the absorption losses in water for the IR light [3] limit the Q-factor to about 10,000. The impact of water absorption losses on the Q-factor value were reported in [2]. Much higher resonance Q-factor values have been achieved, in particular, in 1D PhC configurations, in air [8,9]. The high Q-factor values for the micro-cavity resonances were achieved through the use of a mode-matching approach - by making use of different hole sizes and aperiodic positioning of the holes [9]. The light confinement in such micro-cavities can also be characterized using a classical Fabry-Perot model, in which a guided Bloch mode in a PhC waveguide bounces between the two mirrors that form the micro-cavity [10-12]. When more complex structures involving two micro-cavities or double-cavity structures were introduced, significantly lower Q-factor values resulted [13-15]. The coupled-cavity resonance splitting behaviour was observed to depend on the detailed features of the cavities introduced within the total structure [11, 13].

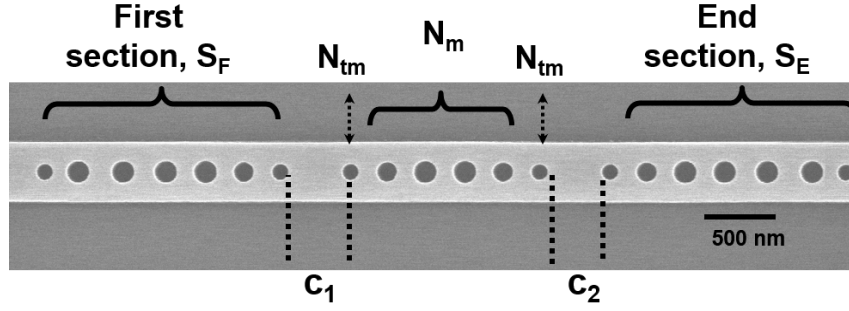


Figure 1: PhC/PhW Coupled cavities separated by two sections  $S_F$  and  $S_E$  with (a)  $N_m$  – Number of periodic mirror holes at mid-section,  $N_{tm}$  = Number of smaller hole replaced or added on the middle section with cavities,  $c_1$  and  $c_2$

The ability to control the strength of optical coupling between two micro-cavities is necessary especially for applications that require a filter response with a nearly level passband and steep skirts at the edges of the pass-band - and optimizing the response may require the use of additional cavities [16].

This paper reports the results of a study on the effects of using different combinations of aperiodic and periodic hole distributions in the mid-section of the coupled cavity structure. It considers the effect of varying the number of periodic holes used,  $N_m$ , located in the mid-section. It also reports on the effect of replacing the periodic holes,  $N_m$ , with smaller holes,  $N_{tm}$ , in the middle section - in order to increase the resonance separation. This approach provides a basic building block for achieving high Q factor resonance in multiple cavity device structures. The impact of the number of periodically spaced mirror holes,  $N_m$ , in each mirror section on the high Q-factor resonance that we have reported previously in [8] is further investigated, after the introduction of two cavities within the outside mirrors, as shown in figure 1. In comparison with our previously reported results [13], a more complete investigation has been carried out - in order to identify the effects of using different combinations of periodic and aperiodic hole structures in the middle, coupling, section of the coupled-cavity structure. The central mirror section separates the two micro-cavities,  $c_1$  and  $c_2$ , as shown in figure 1. We propose that the coupling strength of the two micro-cavities separated by a combination of different holes sizes and spacing can be substantially influenced by the choice of the holes used in the mid-section between the two micro-cavities.

## 2. Device descriptions and simulations results

A micro-cavity design was realized in a planar 500 nm wide photonic wire waveguide with a single row of holes embedded in it. The SOI used in this work consisted of a 260 nm silicon waveguide core supported by a 1  $\mu\text{m}$  thick silica buffer layer. Aperiodic hole tapering was used to provide smooth transitions as light entered the periodic mirror regions from the unstructured waveguide. In the present work, we have investigated the behavior of the free spectral range (FSR) and resonance Q-factor of two-cavity coupled structures by varying the number of holes,  $N_m$ , and using holes with varying diameters in the sections between the mirrors. As shown in figure 1, the cavity end sections,  $S_F$  and  $S_E$ , had nominally identical PhC hole arrangements formed by periodic mirrors, together with four aperiodically located and tapered hole sections within the cavity. The tapered hole structures within the cavity had the same dimensions as were used previously in the single micro-cavity structures [8,9].

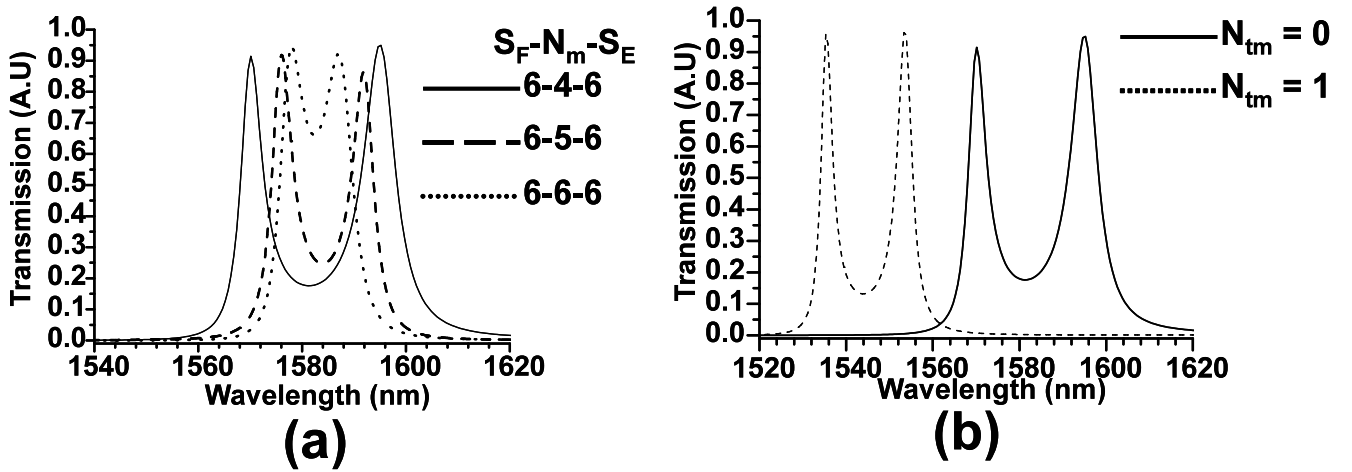


Figure 2: 2D FDTD results for couple cavity with ; (a) a middle section consisting of different periodic hole numbers,  $N_m$  of similar size with  $N_{tm}=0$  (b) a middle section consists of  $N_m = 4$  with different number of smaller holes  $N_{tm}$ .

The middle section consists of a number of periodically spaced holes,  $N_m$ , with diameters of 182 nm and centre-to-centre hole distances of 350 nm – together with tapered sections with a finite number of aperiodic holes,  $N_{tm}$ . For simplicity the hole size within each of these taper sections was kept to have the same nominally identical dimensions as those for the tapered-hole sections,  $S_E$  and  $S_F$ . For  $N_{tm} = 1$ , the holes had a diameter of 131 nm - whereas, for  $N_{tm} = 2$ , the hole sizes used were 166 and 131 nm in diameter, respectively. The same conditions were applied for  $N_{tm}$  of the holes in -the tapered-hole sections,  $S_E$  and  $S_F$ . A two-dimensional (2D) FDTD numerical approach was used to compute the transmission spectra around a wavelength of 1.52  $\mu\text{m}$ . Figure. 2 (a) shows a comparison of the transmission spectra for various numbers of periodic holes,  $N_m$ , but without any aperiodic holes,  $N_{tm}$ , included. As the number of holes in the middle section,  $N_m$ , is reduced from six to four holes, a clear resonance splitting is predicted, implying stronger optical coupling between the two cavities. The free spectral range (FSR) values calculated in the successive cases are 8.89, 15.75 and 24.95 nm, respectively. On the other hand, for the case of four periodic holes,  $N_m = 4$ , where strong inter-cavity coupling was observed previously, the introduction of aperiodic hole sections has resulted in a reduced free spectral range (FSR), as shown in figure. 2 (b). The free spectral range values calculated were 24.95 nm for the case without aperiodic hole sections and 18.28 nm for the case with one-hole tapered sections, respectively. As shown in Fig. 2(b), the transmission spectra are shifted to a shorter wavelength when a tapered section is added to the periodic holes of the  $N_m=4$  mirror. This shift is primarily due to changes in the effective lengths of the different sections making up the entire coupled cavity structure. The difference in FSR values is due to the increase in the number of holes within the middle section - so that stronger light confinement is produced within the cavities. When identically smaller additional holes were introduced within each cavity – denoted by  $N_{tm}=1$ , the normalized transmission spectra of the split-resonance increased by approximately 5% - and more clear splitting of the resonances was also observed.

### 3. Fabrication and experimental results

The devices were fabricated using direct-write electron-beam lithography in a Vistec VB6 machine, together with ICP dry-etching technology. The devices were measured using a tunable laser covering the wavelength range from 1.45 to 1.58  $\mu\text{m}$ . TE polarized light was end-fire coupled into and out of the device waveguides - and the optical signal was then detected using a germanium photodiode.

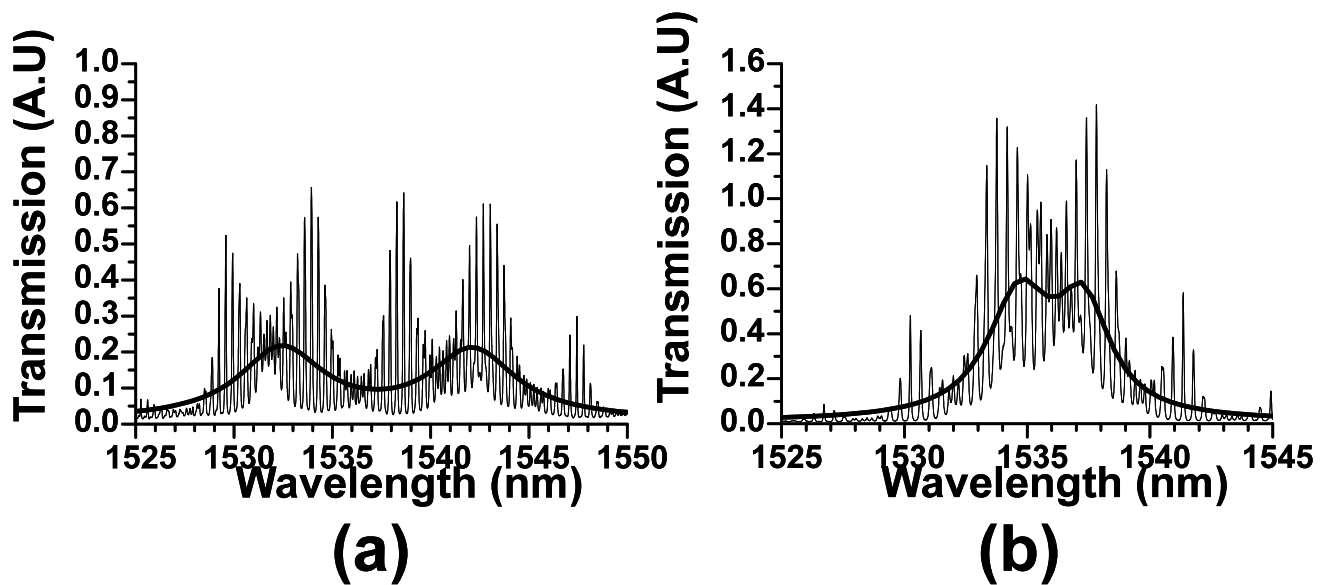


Figure 3: Measured results for coupled cavity structure with  $c_1 = c_2 = 450$  nm and  $N_m = 0$ : (a)  $N_m = 4$  (b)  $N_m = 6$  – corresponding to the simulation results in figure 2(a).

The experimental results were normalized with respect to an identical but unstructured, nominally 500-nm-wide PhW waveguide - without any holes embedded in it. Figure 3 shows the measured transmission spectra for the coupled micro-cavity structures with cavity lengths of 450 nm - and without any taper in the middle section, i.e. where  $N_m = 0$  in all cases – corresponding to the simulated result shown in figure 2 (a). The fine structure that is evident in figure 3 can be attributed primarily to the additional effects of the Fabry-Perot (FP) resonances that occur between the partially reflecting end facets of the sample. The impact of the Fabry-Perot effects produced by the end-facet partial reflections on the resonances is more obvious than for our previous results obtained for single micro-cavity structures. Clearly there is a need to suppress such FP effects in multiple cavity device structures to be used in practical applications. This suppression could be achieved by using suitable thickness anti-reflection (AR) coatings or inverse taper input/output coupling waveguide designs that can reduce the reflected light levels at the end facets. The measured transmission levels of the micro-cavity resonances are shown in figures 3 (a) and (b) for the cases of  $N_m = 4$  and  $N_m = 6$  respectively. The FSR values obtained from the separations between the two resonances were estimated to be approximately 8.01 nm and 2.18 nm, respectively. In order to identify the coupled-cavity resonances in the presence of the strong Fabry-Perot effects due to the sample end facets, commercial software (Matlab) was used to perform lorentzian curve analysis. The results of the analysis are incorporated as the smooth black lines in Fig. 3 (a) and (b). It has therefore been shown experimentally that stronger optical coupling was observed with a reduced number of periodic holes between the two cavities - where, in this case,  $N_m = 4$ . On the other hand, as the number of periodically spaced mirror holes,  $N_m$ , in the middle section is increased, weaker optical coupling is obtained - where the resonances become closer to each other - forming a narrower passband. This is due to the effective length that the light travels through the additional periodic holes in the middle section. It becomes harder to distinguish between the resonances that correspond to the splitting due to the two cavities and the FP effects due to the end facets. It is therefore important to reduce the FP effects, since more clear splitting can then be observed - especially for the weaker optical coupling strength of the two cavities. In order to increase the optical coupling between the cavities and obtain a more pronounced resonance splitting, without the need for additional periodic holes, a combination of periodic and aperiodic hole sequences was introduced - where the number of holes was kept the same – by replacing single holes at each end of the middle section by smaller holes. This change effectively reduce the effective length that light travels within the middle section, as well as smoothing the propagation of the guided mode that enters the middle section.

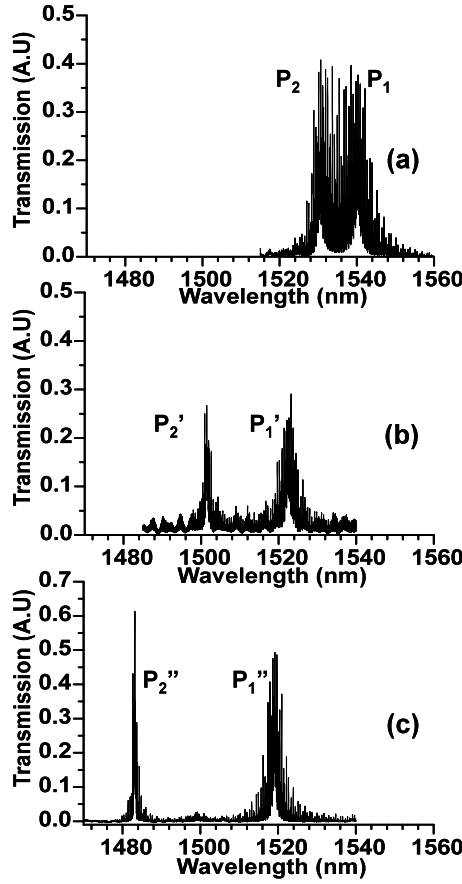


Figure 4: Measured results for coupled cavity structure with  $c_1 = c_2 = 450$  nm and (a)  $N_m = 4$ ,  $N_{tm} = 0$  (b)  $N_m = 2$ ,  $N_{tm} = 1$  (c)  $N_m = 0$ ,  $N_{tm} = 2$  – keeping the middle section with a combination of a total of four periodically,  $N_m$  and/or aperiodically,  $N_{tm}$ , located holes.

Figure 4 shows that, by keeping the total number of holes within the middle sections to four,  $N_m = 4$ , - as the number of smaller holes that are tapered within the middle section,  $N_{tm}$  is increased - the splitting of the two resonances increases. Shifts in the spectral positions of the resonance frequencies from  $P_1$  and  $P_2$  to  $P_1'$  and  $P_2'$  respectively, by approximately 17.59 nm and 3.58 nm, were also observed when the periodic holes in the middle section were replaced by smaller holes – one at each end, where  $N_{tm} = 1$  and  $N_{tm} = 2$ . Furthermore, free-spectral-range (FSR) values of 8.01 nm, 21.26 nm and 35.93 nm were observed for the cases of  $N_m = 4$  ( $N_{tm} = 0$ ),  $N_m = 2$  ( $N_{tm} = 1$ ) and  $N_m = 0$ , ( $N_{tm} = 2$ ), in agreement with the trend of the results obtained using the FDTD approach and shown in figure 2 (a). For instance, more pronounced splitting of the resonances was readily observed for the case of increasing the number of smaller holes,  $N_{tm}$ , in the middle section, while keeping the number of holes constant. For example, as shown in figure 4, when the combination of periodic and aperiodic holes was kept to a total of four holes, the FSR value increased significantly to 35.93 nm, since the periodic holes were replaced completely by smaller holes,  $N_{tm}$ , on each side of the middle section. The resonance Q-factor has also shown a significant increase as the number of periodic holes,  $N_m$ , was reduced and the periodic arrangement was replaced with an aperiodic hole structure,  $N_{tm}$  - as shown in figure 4(a) to (c). The Q-factor values for the case where  $N_m = 4$  and  $N_{tm} = 0$ , as shown in figure 4 (a), were measured to be approximately 200 for  $P_1$  and 300 for  $P_2$  respectively. As for the  $N_m=2$  and  $N_{tm}=1$  cases, as shown in figure 4 (b), the Q-factor values were measured to be approximately 500 and 900 respectively for  $P_1'$  and  $P_2'$ . Finally, for the case of  $N_m=0$  and  $N_{tm}=2$ , the Q-factor values were further increased and were measured to be 700 and 1200 respectively for  $P_1''$  and  $P_2''$ . For instance, as the FSR between the two resonances was increased using the hole arrangement within the middle section, we have seen a significant increase in the Q-factors - which is partly due to the reduction in coupling strength where more clear and isolated resonances

were observed.

In addition, the resonance Q-factor values were reduced significantly for the two cavity condition - as compared with the high Q value achieved previously for the single micro-cavity situation [8]. Carefully designed mode matching hole arrangements are required to retain, at least partially, the Q-factor values, since the Q-factors were reduced, partly because of the increased propagation losses as light enters and propagates within the middle section between the two cavities. In addition, figure 5 shows the variation of the FSR values corresponding to combinations of different numbers of aperiodic and periodic holes used in the middle section. For the case of  $N_m=1$ , the FSR values decreased from 48.36 nm to 4.96 nm as the number of periodically spaced holes,  $N_m$ , increased from 0 to 4. Similar results were observed for each case with  $N_m = 2$  and  $N_m = 3$ , with the FSR values decreasing from 35.93 nm and 17.98 nm to 2.42 nm and 1.55 nm, respectively, as the number of periodic holes,  $N_m$ , was increased.

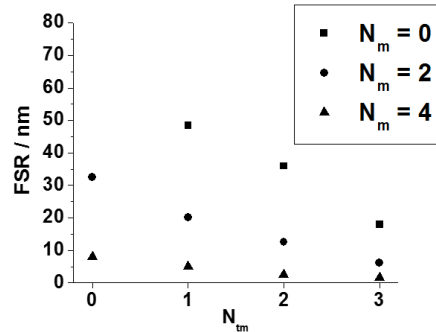


Figure 5: Variation of FSR values in relation with the number of holes in the middle sections - and the number of taper holes used in the middle section/

More pronounced splitting of the two resonances was observed as the number of periodic mirror holes,  $N_m$ , was reduced - while increasing the number of smaller holes (aperiodically spaced and tapered hole sections),  $N_m$  - showing that the two cavity sections were coupled more strongly by reducing the number of periodic mirror holes in the middle section.

#### 4. Conclusions

The free spectral range (FSR) of the resonances of these coupled micro-cavity structures depends strongly on the arrangement of the holes in the middle sections. Stronger separation of the resonances is apparent when the number of periodically arranged holes is reduced or they are replaced by smaller hole sizes within the middle sections. Control of the FSR of the coupled resonator structures, through the use of different combinations of total numbers of periodic mirror sections and tapered aperiodic hole arrangements in the middle section between the cavities, has also been demonstrated. A more pronounced splitting of the resonances, leading to values of the FSR up to approximately 48 nm, was observed with the use of smaller holes in the middle section - which could be useful in optical bio-sensing applications in the infra-red wavelength region.

#### 5. Acknowledgments

This work was supported in part by the Ministry of Higher Education Malaysia (MoHE ) through HiCOE Grant – AKU95.

#### 6. References

- [1] Yang D, Tian H, Ji Y and Quan Q 2013, J Opt. Soc. Am. B, 30, 8, 2027-2031.
- [2] Yang D, Kita S, Liang F, Wang C, Tian H, Ji Y, Loncar M and Qimin Q, 2014 Applied Physics Letter, 105, 063118.
- [3] Chen Y.F, Xavier S, Rupa S, Peg C and Erickson D, 2012, Nano Letter, 12, 1633-1637.
- [3] Joannopoulos J D, Meade R D and Winn J N 1995 Princeton, NJ: Princeton Univ. Press.
- [4] Krauss T F, De La Rue R M and Brand S 1996, Nature. **383**, 699-702
- [5] Cooper J, Glidle A and De La Rue R M 2010 *Optics and Photonics News*. **21** (9) 26-31

- [6] De La Rue R M and Seassal C 2012 *Laser and Photonics Reviews* **6**(4) 564 - 597
- [7] Md Zain A R, Gnan M, Chong H M H , Sorel M, and De La Rue R M 2008 IEEE Photon. Techn. Letters **20** (6)
- [8] Md Zain A R, Johnson N, Sorel M, and De La Rue R M, 2008 Optics Express **16** 12084
- [9] Lalanne P, Sauvan C and Hugonin J P 2008 Laser and photonics reviews, **2**(6) 514-526
- [10] Lalanne P and Hugonin J P 2003 *IEEE J. Quantum Electron.* **39**(11) 1430–1438
- [11] Jin C J, Johnson N P, Chong H M H, Jugessur A, Day S, Gallagher D and De La Rue R M 2005 Optics Express **13**(7) 2295-2302
- [12] Md Zain A R, Johnson N P, Sorel M and De La Rue R M 2009 Electronics Letters **45** (5)
- [13] Md Zain A R, Johnson N.P. Sorel M and De La Rue R M 2010 IEEE Photonic Tech. Letters **22**(9)
- [14] Melloni, A and Martinelli, M.2002 IEEE J. Lightwave Technology,**20** (2) 296–303
- [15] Foubert K, Lalouat L, Cluzel B, Picard E, Peyrade D, Fornel F de, and Hadji E 2009 Applied physics letter, **94** 251111